18

Space Sources of Light

In Chap. 5, we addressed the problems of light and its amazing nature. We discussed the twofold nature of light: wave and particle. As this book regards solar sailing as a non-rocket photon-driven propulsion mode, we shall primarily focus on the properties of solar light and, secondarily, on the light from planets.

The energy of a photon is directly proportional to its frequency or, equivalently, inversely proportional to its wavelength. Frequency and wavelength refer to the oscillations of electric and magnetic fields traveling in a vacuum or inside matter. Wavelength determines the way both fields interact with objects met along their propagation path. Consequently, one can divide the electromagnetic spectrum into regions or bands (with different names). Bands are divided into sub-bands; historically, their nomenclature changed according to the progressive knowledge of their features. Figure 18.1 shows the main regions of the spectrum in terms of wavelength expressed in nanometers (nm), microns (μm), or centimeters (cm), according to the band. Also, some of the sub-band names have been reported. Note how small the visible band is (0.4–0.7 μm) compared to the other regions. It may seem incredible that a typical TV wave transports energy 10^{-12} times that of a photon of 0.1 nm wavelength, namely in the x-ray region. Someone might object that the spectrum regions/sub-regions are somewhat arbitrary. This is only partially true. Although discussing the related criteria is beyond the scope of this chapter, we mention an example: the gamma-ray region includes 511 keV, which corresponds to the energy of the rest mass of the free electron. The wavelength of any photon carrying this energy in vacuum is equal to $\lambda = hc/E = 1{,}239.84191$ nm$/E[eV] = 0.002426$ nm. (In practice, though, neither wavelength nor frequency is suitable for featuring photons beyond the sub-region of the hard x-rays, but energy is appropriate).

Considering the importance of the concepts regarding energy emission from a source of light and the energy received by a surface, we introduce the following definitions:

1. **Source of light:** A source of electromagnetic radiation can be the surface of active sources (like stars, lamps, living hot bodies, gas plasma, etc.) or any surface reflecting/scattering a fraction of the received light. When the source does not appear as point-like, the emitting surface can be partitioned in elemental or infinitesimal surfaces; each is endowed with its own radiation characteristics. Given an oriented surfaced **A**, emitting or receiving energy, and a direction **d** of radiation emission or incidence,

G. Vulpetti et al., *Solar Sails,* Springer Praxis Books,
DOI 10.1007/978-1-4939-0941-4_18

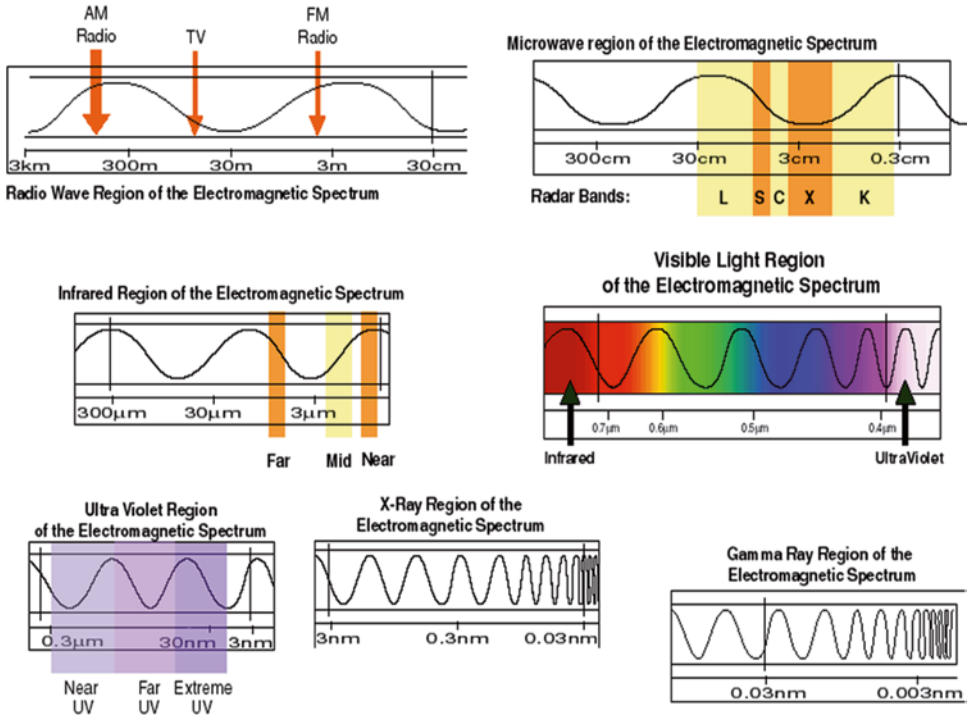

18.1 Regions of the electromagnetic radiation spectrum (Courtesy of NASA)

the angle of emission or incidence between **d** and **n**, the positive normal to d**A**, is denoted by θ (also called the zenithal angle). Thus, the projected or orthogonal-to-**d** area is equal to $dA_n = \cos(\theta)\, dA$, dA being the magnitude of d**A**.

2. **Spectral Radiant Power** (Φ_λ): the power emitted per unit wavelength [W/μm] from a source of light.
3. **Radiant Power**(Φ): is the total power, expressed in watts, emitted by a radiation source. It does not contain any other source-related information. It is equal to Φ_λ integrated from some $\lambda_1 > 0$ to some $\lambda_2 > \lambda_1$.
4. **Spectral Radiant Intensity** (F_λ): the spectral power emitted per unit solid angle about a given direction. $F_\lambda = d\Phi_\lambda / d\omega = d^2\Phi / d\omega\, d\lambda$, usually measured in [W/(sr nm) or W/(sr μm)]
5. **Radiant Intensity** (F): measured in W/sr, it is the F_λ integrated over a broadband [λ_1, λ_2] (as above). It should not be confused with radiance (see below).
6. **Spectral Radiant Exitance** (M_λ): is the spectral radiant power emitted per source's unit area; usually measured in W/(nm m^2).
7. **Radiant Exitance** (M): the power emitted per source's unit surface [W/m^2]. $M = d\Phi / dA$, namely, M_λ integrated over [λ_1, λ_2]. This power is assumed to radiate into the hemisphere that contains **n**.
8. **Spectral Radiance** (L_λ): power emitted by a radiation source per unit wavelength, unit solid angle, and unit *projected* area, namely, $L_\lambda = d^3\Phi / dA_n\, d\omega\, d\lambda$. Spectral radiance

is expressed in [W/(m^2 sr nm)]. Depending on the problem at hand, either photon frequency or energy can be used instead of wavelength.

9. **Radiance** (L): the spectral radiance integrated over a range or band of wavelengths. Radiance units are [W/(sr m^2)]. Radiance should not be confused with the radiant intensity. For a Lambertian surface, L is independent of the viewing direction, by definition; as a result, it comes out that $M = \pi L$.
10. **Spectral Irradiance** (I_λ): is the electromagnetic power per unit wavelength incident on or crossing a unit surface. It is expressed in [W/(m^{2}nm)] or [W/(m^{2}μm)]. $I_\lambda = d^2\Psi/dA d\lambda$, where power Ψ comes from *any* directions in the hemisphere based on d$\mathbf{A}$.
11. **Irradiance** (I): the spectral irradiance integrated over a broadband [λ_1, λ_2]. When the band is the full electromagnetic spectrum, one gets the total irradiance. Irradiance is measured in [W/m^2].

The concepts expressed in the above definitions are compliant with the regulations of the *Commission Internationale de l'Eclairage* (CIE, International Commission on Illumination) for radiometry and photometry. (The latter is radiometry restricted to the visible band, but connected to the spectral sensitivity of the human eye.) In particular, definitions 1–8 address the sources of light, whereas definitions 9 and 10 address radiation received by a surface (even an ideal one). However, a few scientific communities may have adopted different terminology and meanings. For instance, meteorologists call *flux* (as shorthand for *flux density*) the rate of radiant energy passing through a given flat surface, expressed in [W/m^2]. Consequently, they define the incident flux per unit solid angle [W/m^2 sr] as the radiant intensity impinging on a given area.

We use the international conventions and units here. The concepts of spectral and total radiance and irradiance will suffice for our purposes in this chapter.

Like any other source of natural electromagnetic radiation, the Sun does not emit light uniformly over wavelength. Let us consider a unit surface placed at 1 astronomical unit and orthogonally to the sunlight propagation direction, and at zero speed relatively to the Sun; then it is possible to measure the energy that impinges on such area per unit time, totally or as a function of the wavelength. In the former case, one gets the *total solar irradiance* (TSI), whereas in the latter case one obtains the *solar spectral irradiance* (SSI). Figure 18.2 shows SSI, in units of W/(m^2 nm), from 1.5 to 10^6 nm. The sub-regions indicated in the upper part of the figure are detailed in Table 18.1. In other books, you can find some differences in the reported ranges. For instance, the 100 to 400-nm range can be divided into ultraviolet UV-C, UV-B, and UV-A, also according to the health effects on the human body. The ranges reported in Table 18.1 are compliant with the International Standards Organization (ISO) initiative 2002.

From Fig. 18.2 and Table 18.1, one can note some features. *First*, the visible band encompasses most of SSI; *second*, values in the overall UV region are strongly uneven; *third*, SSI decreases monotonically in the full infrared (IR) band; and *fourth*, over 92 % of TSI resides in the [0.4–25] micron range, whereas the UV range captures 8 % of it. Such figures are important in choosing the reflective layer of the sail.

The values of SSI shown in Fig. 18.2 are mean values over three solar cycles (21–23); as a point of fact, SSI values fluctuate in a solar cycle. Such variations are important for Earth's atmosphere, especially in the UV range, inasmuch as its energy content represents

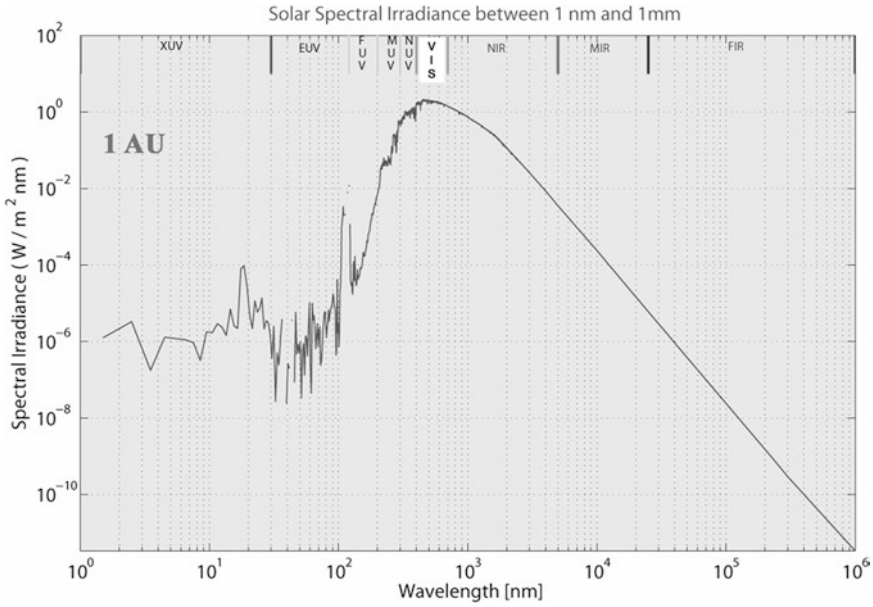

18.2 Sun's spectral irradiance [W/m^2 nm], at 1 AU, over six orders of magnitude in radiation wavelength. Regions have been labeled (Solar Sails, 1st edition of this book)

Table 18.1 Wavelength ranges of some sub-regions of the electromagnetic spectrum.

Fraction of the total irradiance	Sub-region	Min λ (nm)	Max λ (nm)	The following notes refer to the Earth's atmosphere
	XUV (soft x-rays)	1	30	Ionizes atoms and molecules; absorbed in the upper atmosphere
0.06	EUV (extreme ultraviolet)	30	120	Ionizes nitrogen and oxygen molecules; absorbed above ~90 km
	FUV (far ultraviolet)	120	200	Dissociates oxygen molecules; absorbed above ~50 km
	MUV (middle ultraviolet)	200	300	Dissociates oxygen and ozone molecules; absorbed between ~30 and ~60 km
	NUV (near ultraviolet)	300	400	Can reach the ground
0.41	VIS (visible)	400	700	In practice, passes unabsorbed through the full atmosphere
0.529	NIR (near infrared)	700	4,000	Partially absorbed by water vapor
	MIR (middle infrared) or thermal infrared	4,000	25,000 or 50,000	Absorbed and re-emitted by ozone molecules, CO_2, water vapor and the other gases present in low atmosphere
$<5\times10^{-5}$	FIR (far infrared)	25,000 50,000	1,000,000	Fully absorbed by water vapor

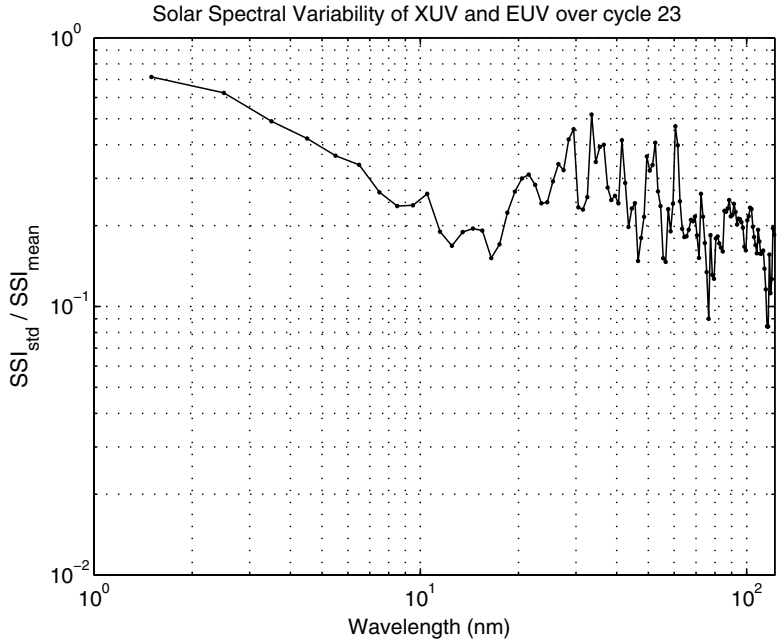

18.3 Variability of SSI in the solar XUV and EUV bands in cycle-23 (author Vulpetti, 2014)

the input of energy to the upper atmosphere: UV photons deposit their energy in the atmosphere layers known as the stratosphere, mesosphere, and thermosphere (altitude increases from the first one). In particular, they make and maintain the ionosphere. In the visible region and in the various infrared bands, relative changes of SSI during a solar cycle are rather small, i.e. of the order of 0.1 % or considerably lower (Chap. 2 of [1]). This is very good for the realization of solar-photon propulsion[1] because the ensuing sailcraft paths can be calculated and predicted with sufficient precision. The scenario changes completely in the UV band, where fluctuations can amount up to 100 % of the means (Fig. 14, page 67 in [1]). Even more happens in the XUV and EUV bands as shown in Fig. 18.3, where the solar spectral variability in these bands is evaluated in terms of standard deviation on average ratio in cycle-23.[2] The 1–120 nm region is not important for obtaining thrust via sail,[3] but it is for sail material degradation, and sail temperature too ([3], Chap. 4).

---

[1] However, for particularly complicated flights such as rendezvous with planets, one can show that the though small fluctuations of TSI have to be taken into account in designing sailcraft trajectories. The entries [5] and (Vulpetti, 2011), added to References of this chapter, are papers advised to the graduate student.

[2] The current solar cycle number is 24, according to the cycle numbering after Carrington, and began in January 2008 (http://solarscience.msfc.nasa.gov/predict.shtml).

[3] The contribution to TSI coming from XUV and EUV regions amounts to about 0.005 W/m^2.

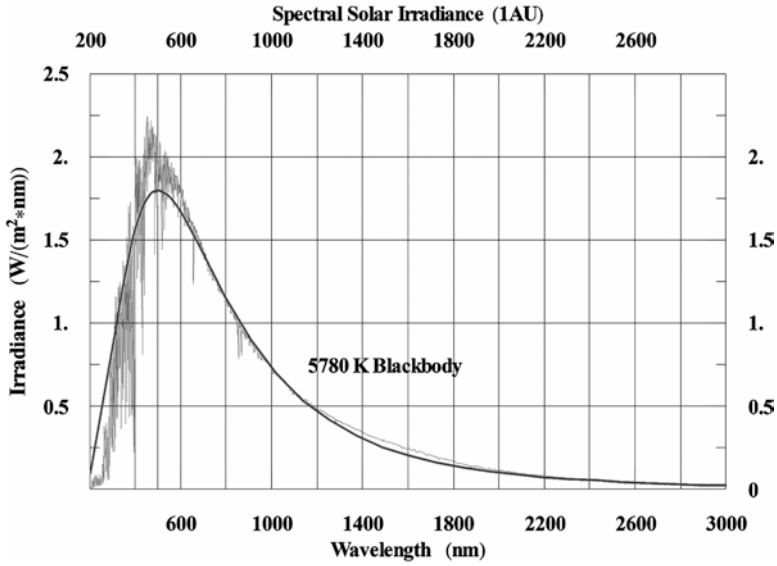

18.4 Solar spectral irradiance (1 AU) from 200 to 3,000 nm; the smooth curve is the blackbody distribution that produces the same total irradiance (approximately 1,370 W/m^2) over the full solar spectrum

From a solar-sail propulsion viewpoint, the above discussion entails that the sail's reflective film has to be chosen for reflecting light of the visible and infrared bands mainly; also, it has to be resistant to ultraviolet photons for decreasing the optical degradation. In Parts I to III of this book, statements like this one are now justified by modern measurement campaigns.

Let us gain additional information about solar light. Figure 18.4 zooms into the central part of Fig. 18.1, namely, from 200 to 3,000 nm. The vertical line represents the observed SSI, whereas the smooth line denotes the spectral radiance, integrated over the solid angle the Sun subtends at the 1 AU (or 6.80×10^{-5} sr), of a blackbody at 5,780 K. Such plots give us some important information:

1. The Sun behaves on average as a blackbody of high temperature, which refers roughly to the photosphere one observes as a whole (but the temperatures of the active solar zones can be much different);
2. The infrared band follows the blackbody distribution pretty well;
3. The visible and ultraviolet bands show non-negligible deviations from the blackbody, especially from the ideal maximum, e.g. ~1.8 W/(m^2 nm) at 500 nm.

Blackbody distribution features a one-to-one relationship between spectral radiance and temperature. In other words, if you know the radiance L_0 of an emitting body (regardless of its real properties) at some wavelength λ_0, there is one temperature T_b distribution passing through the point (L_0, λ_0). A real general emitter can be characterized by a

distribution of blackbody temperatures corresponding to its real radiances values. This is the concept of *brightness temperature* of a real emitting body. In formal terms:

$$T_b = B^{-1}\left(L_0, \lambda_0\right) = \frac{hc/k}{\lambda_0 \ln\left(1 + 2\dfrac{hc^2}{L_0 \lambda_0^{\,5}}\right)} \tag{18.1}$$

where B^{-1} (L_0, λ_0) denotes the inverse of the Planck function describing the blackbody spectral radiance (which can be found in any textbook on electromagnetic radiation). In Eq. (18.1), c, h, and k denote the speed of light in vacuum, and the Planck and Boltzmann constants, respectively. Figure 18.5 shows the brightness temperature of the Sun in the 200 to 3,000-nm range (the same of Fig. 18.4). In this range, the Sun looks like a set of blackbodies from 4,000 to 6,450 K. Note, comparing Figs. 18.4 and 18.5, how small deviations in radiance at longer wavelengths translate into significant changes of the brightness temperature with respect to the reference blackbody temperature. This is expressed in the rightmost part of Eq. (18.1).

Now it's time to answer the following question: If a solar sail is R (usually astronomical units) away from the Sun, what is the total solar irradiance on it? Denoting such irradiance by I (R, **p**), one can write

$$I\left(R, \mathbf{p}\right) = I_{1\mathrm{AU}}\, f\left(R, \mathbf{p}\right) \tag{18.2}$$

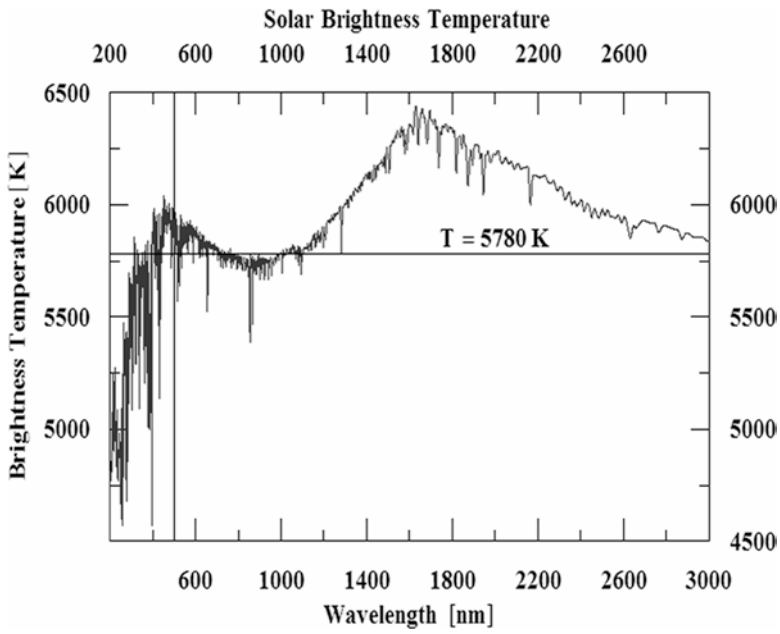

18.5 Solar brightness temperature from 200 to 3,000 nm

where the first term on the right-hand side is the standard TSI, whereas the second term represents the scaling function. The set of parameters the scaling factor depends on has been denoted by **p.** Figure 18.6 shows the behavior of TSI in the solar cycles 21–23. The gray lines plot the daily averaged values coming from the radiometers on board satellites. The black line comes from data smoothing. Such a figure is the composite TSI time series, made by PMOD, which unifies measurements from different radiometers and histories (i.e., including degradation), and is adjusted to 1 AU. TSI, also named the solar constant, is not a constant; this quality jump—fully related to the space era—began on November 16, 1978, by means of the Hickey-Frieden (HF) radiometer on the satellite Nimbus-7. Subsequently, other high-precision satellite radiometers have measured the total solar irradiance every 2–3 min. The radiometers of the experiment VIRGO on the spacecraft SOHO have been continuing to monitor the Sun. French microsatellite Picard and NASA's large Solar Dynamics Observatory (SDO, under the Living-with-a-Star program) were launched for new long high-accuracy and high-resolution campaigns of solar radiation

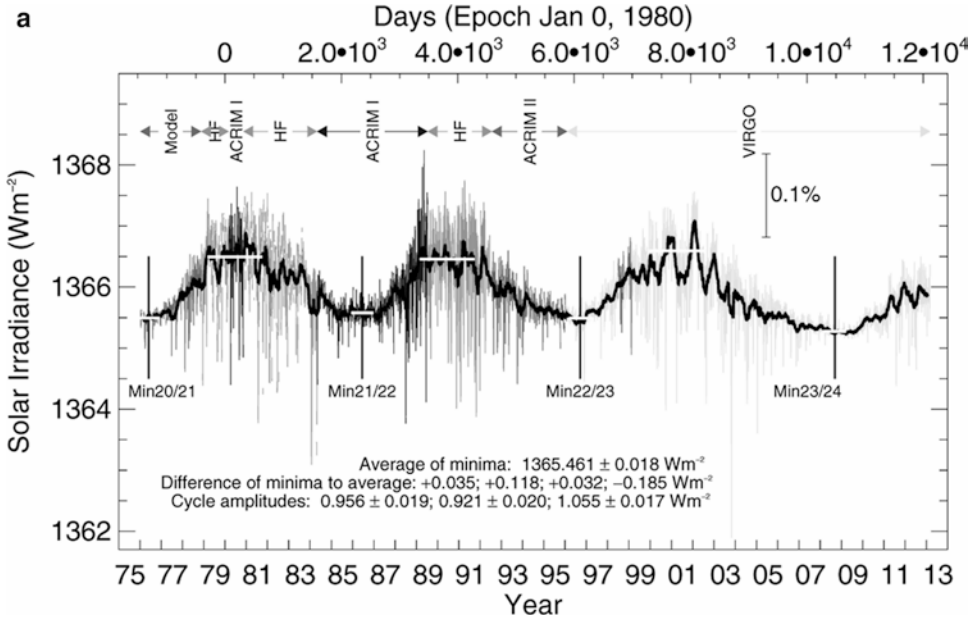

18.6 (**a**) Total solar irradiance (TSI, adjusted at 1 AU), over the solar cycles 21 to 23, and the new cycle 24 up to February 2013. The *gray lines* are the composite daily averaged values from many satellite observations. The *solid black curve* represents data smoothing. Note that the cycle amplitudes are lower than 1 W/m^2. Space-borne data of TSI show that the "solar constant" is not constant. (Courtesy of PMOD, World Radiation Center, Switzerland). (**b**) Recent TSI measurements, in the 2003–2014 period, from the instrument Total Irradiance Monitor (TIM) onboard NASA's spacecraft named Solar Radiation and Climate Experiment (SORCE), according to [7] (Courtesy of the American Geophysical Union)

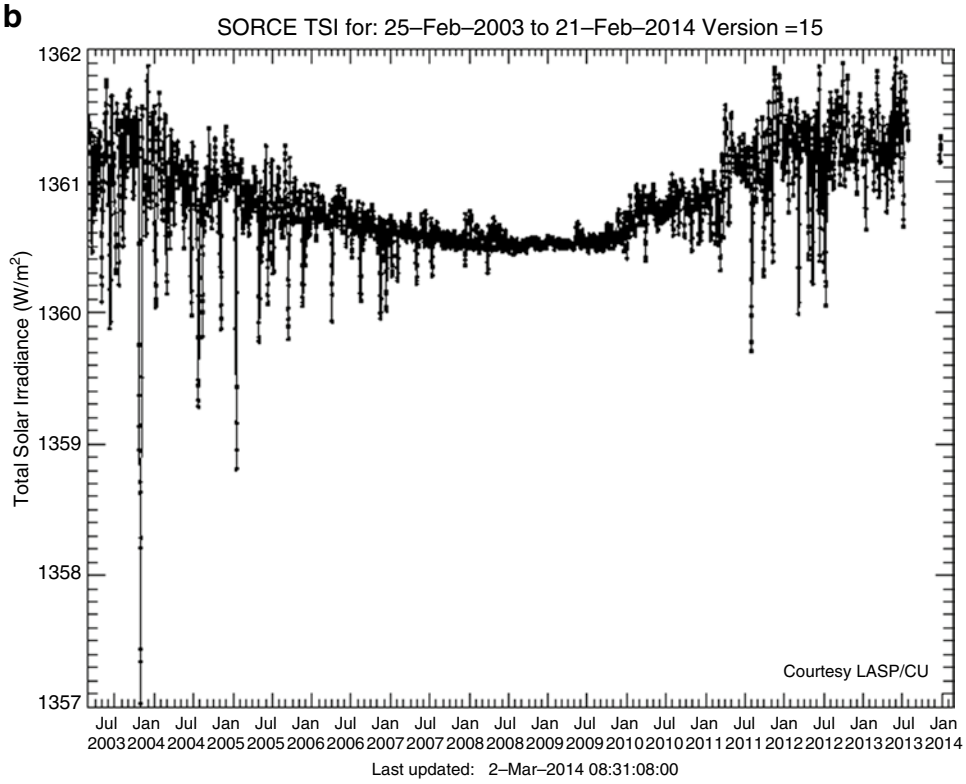

18.6 (continued)

measurements for better understanding the complex solar activity cycle. Forecasting TSI over the next years is a difficult task indeed. However, time series such as those ones plotted in Fig. 18.6a, and the new models of the upper solar layers—where the solar variable magnetic field plays a prime role—may greatly help solar-physics scientists in this job. An excellent review of these important topics can be found in [4].

In the models of Earth climate, a TSI value of $1{,}365.4 \pm 1.3$ W/m^2 is standard. However, according to Kopp and Lean [7], recent measurements from the instrument Total Irradiance Monitor (TIM) onboard NASA's spacecraft named Solar Radiation and Climate Experiment (SORCE), show a TSI mean value of $1{,}360.8 \pm 0.5$ W/m^2. This discrepancy (-4.6 W/m^2) is remarkably high not only for the strong implications on Earth climate (a huge problem nowadays), but also for accurate solar-photon sailing trajectories.

Nevertheless, in this book, we will go on referring to 1,366 W/m^2 as the mean value of TSI over three solar cycles (21–23), also because, in literature, other time series (coming from other satellite instruments) regarding TSI continue to be endorsed.

For a sailcraft, variable TSI perturbs trajectory with respect to the assumed TSI-constant profile. The closer one goes to the Sun, the higher is the TSI impact. If one swings by the Sun, the trajectory arcs approaching the Sun may extend from some weeks to a few

months; since there are daily TSI fluctuations, even of 3–4 W/m^2, the outbound trajectory arc profile changes with respect to that with no TSI change, depending on the flyby perihelion value. This should apply in particular to the velocity direction. If the sailcraft deviates of 1 arc-minute at 1 AU, this translates in a miss distance of 1.75 million km at 40 AU. If one is trying to fly by Pluto or another object of the Kuiper belt, this error could means the partial failure of the mission. One may object that deviations like this one (or even greater) could be corrected. However, a sailcraft receding from the Sun after a flyby is endowed with very high speed; it could take less than 2 weeks to pass Earth orbit, depending on perihelion and lightness number values. In other words, time for correction is short while the solar pressure decreases rapidly. This is only one of the several trajectory error sources influencing the trajectory of a sailcraft after a solar flyby. Besides the obvious attitude control uncertainties, we have to know how the space environment changes the thermo-optical properties of the sail's reflective and emissive films. Thrust acceleration and sail temperature depend on these properties, as we shall see in Chap. 19.

Greatly affected by variable TSI are the planetary rendezvous missions; the case for Mars has been analyzed recently [5, 6]. In any case, as solar sailing is a continuous photon propulsion mode, the irradiance from the external source(s) has to be modeled accurately for any mission. This means that when a mission design is performed, one should do a sensitivity analysis, also to address our ignorance in predicting TSI in future years. Another potential question regarding TSI is its claimed isotropy. Now, we have no long-period measurements of TSI at high heliographic latitudes. The time series of Fig. 18.6 are measurements substantially on the ecliptic, namely between −7.25° and 7.25° with respect to the solar equator.

From studies in recent years, most of the TSI fluctuations appear to be explained by the change of luminosity in sunspots and faculae. With respect to the mean photosphere temperature, faculae are brighter and sunspots are darker. Thus, when the number of sunspots augments, the solar irradiance increases. One should note that the actual explanation of this fact is much more complicated [4].

Now let us discuss the scaling factor in Eq. (18.2). We know that a general point-like source of natural light emits spherical waves. As a result, if we observe the Sun far enough, we can write $f(\mathrm{R}, \mathbf{p}) = 1/R^2$ (where R is expressed in AU), namely, the scaling factor depends on the distance. What happens if the sail is sufficiently close to the Sun? We have two combined effects.

The *first* consists of a reduction of the solar irradiance with respect to the $1/R^2$ law caused by the finite size of the Sun as observed from the sailcraft at a distance R. As a point of fact, each elementary area of the Sun casts its light onto the sail according to the area-sail direction. Even assuming that the Sun radiance is uniform (actually, it is not so), there is a spread of the radiation impinging on the sail. This reduces the solar pressure compared to the inverse-square law. In 1989, C.R. McInnes and J.C. Brown published $f(R, \mathbf{p})$ for a perfectly reflecting at-rest flat sail oriented radially. In 1994, author Vulpetti calculated the effect on an arbitrary-oriented moving flat sail. Although the general solution is in closed form, it is notably complicated, and its proof is quite beyond the scope of this book. The former solution is a particular case of the latter one. The main feature of such irradiance reduction is that the deviation from the ideal R^{-2} law is negligible above 0.1 AU

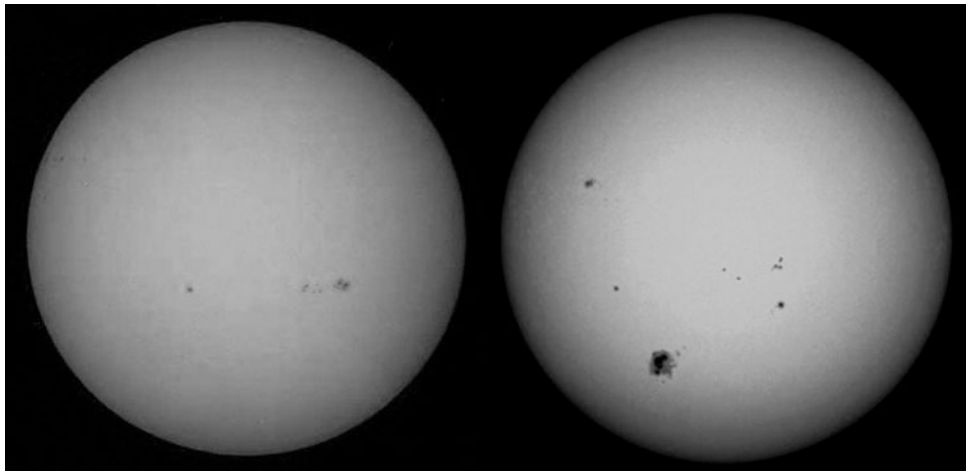

18.7 Pictures of the solar photosphere showing sunspots and the limb-darkening effect (Courtesy of NASA)

(or about 21.5 solar radii). In particular, at 0.2 AU, such deviation is also lower than the irradiance reduction caused by the sunlight aberration on the sail. The *second* reduction in solar pressure can be seen by Fig. 18.7, showing two images of the photosphere in the visible band. One can immediately note that the observed solar radiance is not uniform over the solar disk. In particular,

1. The solar brightness decreases from the center to the disk edge or the limb;
2. Radiation tends to redden as the observer progressively looks toward the limb.

The overall phenomenon is referred as *limb darkening* and addresses the solar photosphere as a whole. As a point of fact, as the Sun is not uniform in its properties, in particular, temperature is height-dependent; however, for a number of emission spectral lines one may observe the opposite of the above points, i.e. limb brightening. The contribution of such lines to the effective TSI is negligible for propulsion purposes.

Describing limb darkening quantitatively is not a simple task, as the local and general properties of the external layers of the Sun are quite complicated. However, if one assumes thermodynamic equilibrium and solar emissivity constant over the whole electromagnetic spectrum, the so-called graybody approximation, one can get a particularly simple expression of the total radiance as function of the observer's zenithal angle as follows:

$$L(\theta) = L(0)\frac{3\cos\theta + 2}{5} = \langle L \rangle \frac{3\cos\theta + 2}{4} \tag{18.3}$$

where $L(0)$ denotes the total radiance measured along the line of sight, and $<L> = 20.09$ MW/(m^2 sr) is the mean solar radiance. There are other more accurate models of limb

darkening. For instance, in recording images of the photosphere via special solar telescopes such as the solar bolometric imagers, the following model is used for limb darkening:

$$L(\theta) = L(0)\left(a_0 + a_1 \cos\theta + a_2 \cos^2\theta + \ldots\right) \tag{18.4}$$

where the actual number of terms is found via regression analysis.

With regard to the combined effect from finite size and limb darkening onto a general-attitude sail, some simplified formulas can be found in Chap. 4 of NASA/CR 2002-211730, June 2002, which can be downloaded from http://www.giovannivulpetti.it/.

When a deployed sailcraft orbits Earth for weeks or months, depending on its lightness number, its trajectory is further perturbed by the radiation emitted from Earth. Also, if ever a sail-based transportation system were operational back and forth between the L1 and L2 points close to the Moon, then the sail motion would be perturbed by the lunar radiance. In both these cases, irradiance on the sail depends also on the changing Earth/Moon phases the sailcraft sees along its orbit. In the much more complicated case of sailcraft orbiting Earth at low altitude, one should take into account global cloud coverage, and the thermal emission from much different sources such as continents and oceans. If a sailcraft spirals for long time, the different components (which can be calculated as function of time) of the irradiance should be averaged; but this task should be accomplished after the basic thrust validation in a real flight.

As a simple exercise, we can compute a rough approximation of the Earth-caused irradiance on a sail at the geostationary altitude:

1. Let us consider the zenith emission via Earth's cloud- and aerosol-free atmosphere approximation. Earth surface, as a whole, may be assumed to be a blackbody emitter at 288 K (its radiance peak, at 10 μm, lies in the infrared region). In the near and thermal infrared regions, combining radiance and transmittance gives an interesting result: although the atmosphere transmission exhibits a complex "indented" behavior and swings many times between almost zero (full opacity) and almost 1 (full transparency), nevertheless the only range with appreciable energy emission to the outer space is 8–13 μm. Such a window encompasses 31.2 % of the total surface emission, whereas we can assume roughly 60 % of mean atmospheric transmittance. Thus, if the sail is at a distance r from the Earth barycenter ($r = 6.61$ earth radii in this example), the thermal irradiance on the sail amounts to

$$I_{\mathrm{IF}} \cong \sigma T_{earth}{}^4 \xi_{8-13} t_{\mathrm{IF}} / r^2 = 1.67\,\mathrm{W/m^2} \tag{18.5}$$

where σ, ξ_{8-13}, and t_{IF} denote the Stefan-Boltzmann constant, the power fraction emitted in the 8 to 13-μm range, and the mean atmospheric transparency in the same range, respectively. Expression 18.5 neglects the emissions from the different layers of the atmosphere and their related absorptions before exiting the full atmosphere.

2. Let us turn to the visible and near-infrared light (V-NIF or the 0.4 to 4-μm range) originating from the Sun and reflected by Earth. Although things are very complicated, we can use the observed quantity known as the *planetary albedo.* Let us summarize. *Bond albedo* is defined as the total energy reflected from an object on which solar light impinges. If the object is a planet, then one gets the planetary albedo. For Earth, sunlight reflection depends strongly on water, snow/ice, vegetation, desert, clouds, human settlings, and so forth. In addition, Earth's albedo changes with latitude and regional mean surface temperatures (that affect the snow/ice extensions). When Earth's albedo is averaged over latitude/longitude, height from ground, and over 1 year, one gets the mean planetary albedo (here denoted by A_p), a useful quantity indeed. The V-NIF-related irradiance onto a sail can then be approximately by

$$I_{\mathrm{V-NIF}} \cong \frac{1}{4} A_p \xi_{0.4-4} \,\mathrm{TSI} / r^2 = 2.20\,\mathrm{W/m^2} \tag{18.6}$$

where TSI = 1,366 W/m^2 (which is the mean value of the daily means in the solar cycles 21–23, included in Fig. 18.6), $A_p = 0.31$, and $\xi_{0.4-4} = 0.91$ (the fractional solar irradiance at 1 AU in the V-NIF range); such values come from observations. The factor ¼ stems from the maximum cross section on the spherical surface ratio.

Thus, at 1 AU from the Sun, the terrestrial irradiance onto a sail at a geostationary radius amounts to 3.9 W/m^2, according to this approximate model. This is a factor 3 of the mean TSI cycle amplitudes observed since 1978 (Fig. 18.6).

We have to note that the inverse-square law used in Eqs. (18.5) and (18.6) is not fully correct. For shorter distances, the finite-size of Earth intervenes heavily in the computation of the irradiance. The full calculation is considerably more complicated than the solar case; as a matter of fact, as the sail draws closer to Earth, it can "distinguish" the various regions (including the atmosphere) of the planet with their own radiative characteristics. The changing attitude of a sailcraft orbiting the Earth entails that, alternatively, the front-side, the backside, or both sides of the sail are irradiated in complicated configurations. For a real sailcraft to be operational around our planet, one may test whether the full irradiation model is sufficiently correct, and how to improve it via the orbit determination process. Figure 18.8 shows some climatological quantities of our globe averaged in April 2014. They all affect the net radiation from the various zones. The reader can, even at a glance, realize how complicated the radiation from Earth's surface and atmosphere may be.

Finally, let us note that the solar irradiance changes according to Earth's orbit radius. As the osculating Earth orbit has a mean eccentricity of 0.0167, irradiance at the top of Earth's atmosphere varies from 1,321 to 1,413 W/m^2. Such change affects Eqs. (18.5) and (18.6) the same way; as a point of fact, $\sigma T_{\mathrm{earth}}{}^4$ is proportional to TSI.

We have shown how is delicate the matter of computing the irradiance on the sail area. We note again that this is the amount of radiation received by the sail *before* it interacts with photons. Chapter 19 describes the interaction in a simplified way.

Acknowledgments We thank Dr. Robert F. Cahalan, head of the Climate & Radiation Branch of NASA's Goddard Space Flight Center, for his *Mathematica* notebook *SolarIrr-3.nb* on solar and terrestrial irradi-

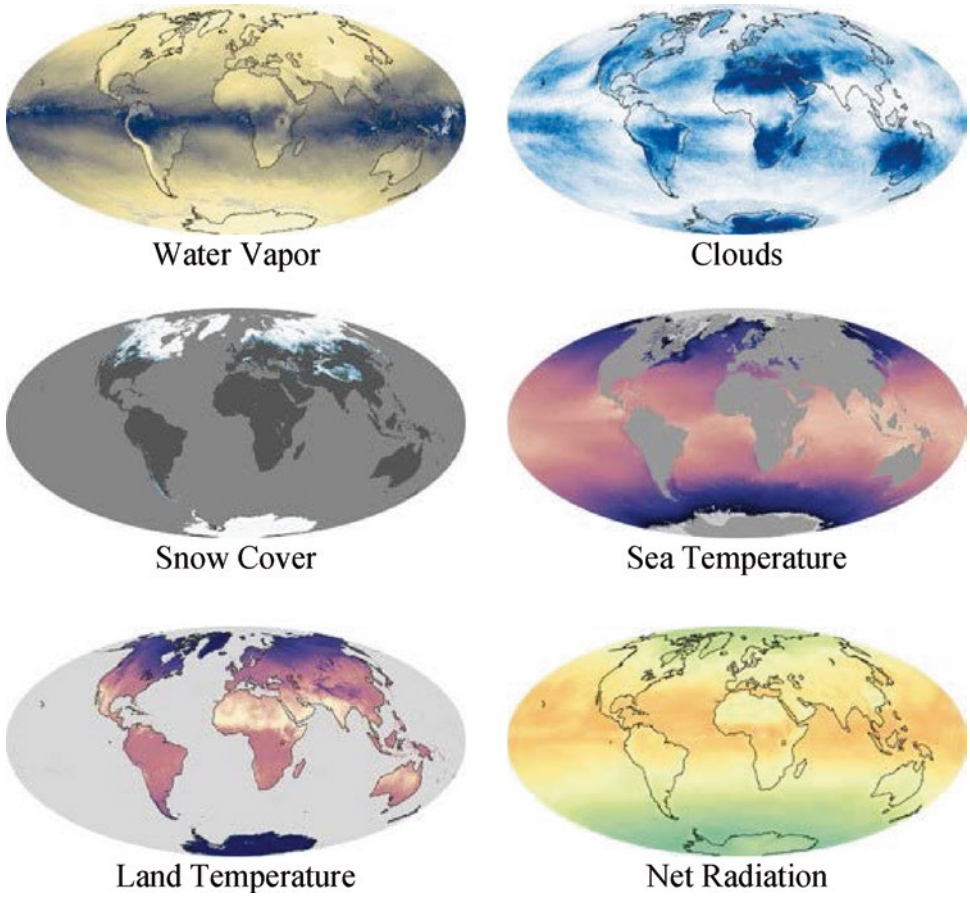

18.8 Some meteorological/climatological quantities throughout an Earth surface map in April 2014 (Courtesy of NASA)

ances, on which we based Figs. 18.2, 18.4, and 18.5. Special credit goes to Physikalisch-Meteorologisches Observatorium, Davos, Switzerland, designated to serve as a world radiation center since 1971, for the composite TSI time series, shown in Fig. 18.6.

FURTHER READING

http://climate.gsfc.nasa.gov/.
http://www.pmodwrc.ch/.
http://umbra.nascom.nasa.gov/sdac.html; http://sohowww.nascom.nasa.gov/.
http://www.gigahertz-optik.com/database_en/html/applications-tutorials/.
http://www.optics.arizona.edu/Palmer/rpfaq/rpfaq.htm.

http://www.solarmonitor.org/index.php.
http://www.albedoarts.net/Define.html

REFERENCES

1. J. P. Rozelot (Ed.), *Solar and Heliospheric Origins of Space Weather Phenomena*, Lecture Notes in Physics Series, Springer-Verlag Berlin Heidelberg, 2006(recommended for the graduate student)
2. J. M. Palmer, B. G. Grant., *The Art of Radiometry*, SPIE Press Monograph, PM184, December **2009**
3. G. Vulpetti, *Fast Solar Sailing – Astrodynamics of Special Sailcraft Trajectories*, Space Technology Library, Springer, August **2012**
4. V. Domingo, I. Ermolli, P. Fox, C. Frohlich, M. Haberreiter, N. Krivova, G. Kopp, W. Schmutz, S. K. Solanki, H. C. Spruit, Y. Unruh, A. Vogler, *Solar Surface Magnetism and Irradiance on Time Scales from Days to the 11-Year Cycle*, Space Science Review,**2009**
5. G. Vulpetti, *Effect of the total solar irradiance variations on solar-sail low eccentricity orbits, Acta Astronautica*, Vol. 67, No. 1-2, July/August **2010**
6. G. Vulpetti, *Total solar irradiance fluctuation effects on sailcraft-Mars rendezvous*, Acta Astronautica, Vol. 68, No. 5-6, March/April **2011**
7. G. Vulpetti, *Impact of Total Solar Irradiance Fluctuations on Solar-Sail Mission Design*, SciTopics, November **2010** (an overview of the problem).
8. G. Kopp and J. L. Lean, *A new, lower value of total solar irradiance: Evidence and climate significance*, Geophysical Research Letters, Vol. 38, L01706, doi:10.1029/2010GL045777, **2011**